Chinese Journal of Physics 88 (2024) 768–785

Contents lists available at ScienceDirect

Chinese Journal of Physics

journal homepage: www.elsevier.com/locate/cjph

Quantum thermodynamics of the charged AdS black hole with nonlinear electrodynamics field

R.H. Ali [a], B. Pourhassan [b,c,d,*], G. Mustafa [a]

[a] Department of Mathematics, The Islamia University of Bahawalpur, Bahawalpur, Pakistan
[b] School of Physics, Damghan University, Damghan, 3671641167, Iran
[c] Center for Theoretical Physics, Khazar University, 41 Mehseti Street, Baku, AZ1096, Azerbaijan
[d] Centre of Research Impact and Outcome, Chitkara University, Rajpura-140401, Punjab, India

ARTICLE INFO

Keywords:
Black hole
Thermal fluctuation
Logarithmic correction
Exponential correction
Phase transition

ABSTRACT

In this paper, we investigate the thermodynamic properties of an AdS-charged black hole coupled with a nonlinear electrodynamic field, taking into account the effects of thermal fluctuations. Our analysis focuses on how thermal fluctuations impact the entropy of the black hole. It is known that at the quantum level, thermal fluctuations bring about changes in the entropy of a black hole in both exponential and logarithmic ways. We present the logarithmic and exponentially corrected thermodynamic characteristics of the black hole, such as Helmholtz free energy, pressure, enthalpy, Gibbs free energy, and specific heat. A comparative analysis of equilibrium states with corrected thermodynamic potentials is conducted to observe the significant influence of the black hole under consideration. Additionally, we examine a second-order phase transition in the case of non-perturbed correction.

1. Introduction

The Bekenstein–Hawking area law for black hole (BH) entropy was found by using the quantum approach [1] and string theory [2], which has brought back interest in the quantum aspects of BH physics. The profound interactions between the physics of BHs and the fundamental principles of thermodynamics were initially elucidated during the early 1970s, as documented in the seminal works [3–5]. The underlying framework of this phenomenon is deeply connected with the complex structure of gravitation, which is crucial in establishing the entropy of BHs [4,6,7]. Additionally, the principles of quantum mechanics determine that BHs emit radiation and possess a finite temperature [5,8]. Thermodynamics, being situated at the intersection of the gravitational and quantum frameworks, is often regarded as a portal through which one can gain insights into the fundamental principles underlying the quantum theory of gravity [9]. The study of BH thermodynamics is of great importance to the progress of quantum field theory in the context of curved space–time. According to our comprehension, BHs exhibit a profound association with the fundamental laws of thermodynamics and can be considered entities characterized by a maximum entropy [10,11]. It was postulated that the entropy of BH was strongly linked to the surface area of its BH radius rather than its volumetric properties. Theoretical physicists believed Planck-scale thermal fluctuations could change the area-entropy relationship of a BH. Furthermore, these phenomena can be further investigated and comprehended through the application of the holographic principle, as discussed in [12,13]. It is worth noting that in these proposed modifications, the entropy continues to exhibit scaling behavior that is dependent on a certain function of the area. The quantum corrections to space–time would modify the entropy area law. The quantum correction through thermal fluctuations refers to two types of corrections: perturbed correction, also known as a logarithmic correction (at leading

* Corresponding author at: School of Physics, Damghan University, Damghan, 3671641167, Iran.
E-mail addresses: hasnainali408@gmail.com (R.H. Ali), b.pourhassan@du.ac.ir (B. Pourhassan), ghulam.mustafa@iub.edu.pk (G. Mustafa).

https://doi.org/10.1016/j.cjph.2024.02.020
Received 18 November 2023; Accepted 14 February 2024
Available online 17 February 2024

order [14]), and non-perturbed correction, also known as an exponential correction [15]. In various settings, both perturbative and non-perturbative corrections have received extensive scholarly attention. The story is as follows: when black hole size reduced due to the Hawking radiation, perturbative correction become dominant. Reducing more in size yielding the black hole to the Planck size where non-perturbative corrections become dominant. It is been proposed that correction terms are universal and have the approximate form [15],

$$S = S_0 + \psi \log S_0 + \cdots + \lambda \exp(-S_0) \tag{1}$$

where ψ and λ are correction coefficients, and dots denote higher-order corrections [16]. It was found that perturbative corrections of AdS BHs exist, as evidenced by the Refs. [17–21]. The utilization of the extremal limit of BHs was used for acquiring perturbative corrections, as revealed in the works of [22,23]. It has been suggested that the aforementioned corrections can be derived through an analysis of the density of microstates within a conformal field theory [24]. In [25], the quantum correction to the Cardy formula for BHs was used to derive the logarithmic correction. Black hole entropy modifications have been calculated using the Rademacher expansion [26]. Because of this, a lot of research has been done using many diverse methodologies to look at perturbative corrections to the entropy of a BH [27,28]. The entropy of BHs that exceed the Planck scale is directly proportional to the area of their event horizon. However, it is necessary to make corrections to this relationship when considering relatively smaller BHs. When the BH is shrunk, it is essential to study leading-order corrections to entropy. The influence of quantum fluctuations near the equilibrium state becomes considerable in the case of BHs and contributes to affecting the entropy of the BH. These modifications, which are regarded as the quantum effect and are caused by quantum fluctuations, change the holographic principle [29–31]. Kaul and Majumdar [32], have made significant contributions to the field of quantum correction geometry. Specifically, they have focused on determining the simplest corrections to the Bekenstein area entropy relation. It is discussed in [33] that the Hawking temperature increases unboundedly with the mass of a BH, as predicted by the leading-order correction to the geometry of such objects in four-dimensional Einstein gravity with a negative cosmological constant. Current efforts [34–37], focus on the research of logarithmic modifications in a variety of contexts. In order to take a Schwarzschild BH in a cavity of small radius, a logarithmic correction term must be present [38]. For different BHs geometries, it has been noted that these modified logarithmic terms are significant [39–56,56]. Recently, Abbas and Ali [57–59], have made contributions to the field of first-order logarithmic correction using thermal fluctuations.

The exponentially corrected or non-perturbed correction term arises when performing microstate counting exclusively for quantum states on the horizon [60]. The investigation into the microscopic origins of entropy is an important area of study in the field of quantum BH physics. The Bekenstein–Hawking area law for entropy is a standard requirement for any quantum theory of BHs. Both string theory and loop quantum gravity provide a framework for microstate counting, which not only confirms the Bekenstein–Hawking area law but also introduces additional corrections. The quantum description of BH horizons is a key aspect of our method that will be essential in our derivation.

In recent times, a novel exponential term has been postulated in order to modify the entropy of BHs. It has been speculated that the quantum theory of gravity may provide results similar to the exponential corrections in the entropy of BHs. Till now, a comprehensive thermodynamic analysis of BHs, including exponential entropy corrections, has been absent in the literature, except for the notable work presented in [61]. Consequently, this paper aims to address this gap by conducting such an analysis for various significant BH configurations. Non-perturbative methods emerge themselves through exponential corrections in the theoretical framework [62–64]. The most captivating scenario arises from the exponential term that exhibits non-perturbative dominance [64–67]. Recently, Pourhassan et al. [68,69], conducted a comprehensive analysis on the universality of these corrections, which exhibit logarithmic and exponential correction. Furthermore, they investigated the effects of these quantum corrections on black holes thermodynamics.

The universal impacts of non-linear electrodynamics (NLED) theory have been extensively studied in order to investigate the problem of universal evolution, as indicated by the Born–Infeld theory [70–72]. The impact of NLED in cosmology has been highlighted by a recent study, specifically in relation to the transition time of both large and small areas. In recent years, NLED containing cosmological models have received a great deal of attention [73–75]. Research on the NLED in heavenly bodies has grown due to significant results [76–79]. The surprising nature of Einstein's solutions for gravity and the NLED field becomes apparent when considering them in the context of the Big Bang. Nonlinear electrodynamic fields may play an essential role in the universe. In order to comprehend these solutions, one needs to understand the correlation between strong magnetic and electromagnetic nonlinear fields. Previous studies [80–84] have examined BHs with multiple horizons in NLED fields. Gunasekaran et al. [85], conducted a study on the thermodynamics of charged BHs, considering the influence of NLED. They also examined the critical behavior of charged BHs. Recently, Abass and Ali [57], discussed the extended phase space thermodynamics of BH with NLED field and analyzed the thermodynamic properties and critical exponents. Mazharimousavi [86], formed the RN-BH solution coupled with NLED field. The objective of this study is to examine the thermodynamic properties of a NLED BH through thermal fluctuations.

The paper is organized as follows: In Sec. 2, we review the considered BH solution. In Sec. 3, we studied equilibrium thermodynamic characteristics. Section 4, presents the quantum corrected thermodynamics of the BH with logarithmic corrected entropy. Section 5, discusses the corrections in thermodynamics of this BH due to exponential correction entropy. Results are summarized in the last section.

2. Review of the NLED black hole solution

The NLED model will be integrated with Einstein's gravity by means of the action described in [86],

$$S = \int d^4x\sqrt{-g}\Big(\frac{1}{16\pi G}R + \mathcal{L}(\mathcal{F})\Big), \tag{2}$$

where R is the Ricci scalar, G is the Newton gravitational constant, $\mathcal{F} = \frac{1}{4}F_{\mu\nu}F^{\mu\nu}$ is the Maxwell invariant [86], and $\mathcal{L}$ is NLED Lagrangian, which is given by,

$$\mathcal{L} = -\mathcal{F}\frac{16\left(3\sqrt{-2\mathcal{F}} + \zeta(\zeta + \sqrt{\zeta^2 + 4\sqrt{-2\mathcal{F}}})\right)\sqrt{-2\mathcal{F}}}{3(\zeta + \sqrt{\zeta^2 + 4\sqrt{-2\mathcal{F}}})^4}, \tag{3}$$

where ζ is an NLED parameter. The Einstein field equation can be written as

$$G^{\nu}_{\mu} = 8\pi T^{\nu}_{\mu}, \tag{4}$$

where G^{ν}_{μ} is the Einstein's tensor and T^{ν}_{μ} be energy momentum tensor. The NLED energy momentum tensor is of the form [86],

$$T^{\nu}_{\mu} = \frac{1}{4\pi}(\mathcal{L}\delta^{\nu}_{\mu} - \mathcal{L}_{\mathcal{F}}F_{\mu\gamma}F^{\nu\gamma}), \tag{5}$$

where $\mathcal{L}_{\mathcal{F}} = \frac{\partial\mathcal{L}}{\partial\mathcal{F}}$.

The consistency of the Einstein field equations has been established [86]. It is worth noting that there is only one radius involved in this scenario, which yields

$$G^0_0 = 8\pi T^0_0, \tag{6}$$

The following is the form of the spherically symmetric ansatz metric.

$$ds^2 = -h(r)dt^2 + \frac{1}{h(r)}dr^2 + r^2(dr^2 + \sin^2\theta d\phi^2), \tag{7}$$

where,

$$h(r) = 1 - \frac{2m}{r} + \frac{Q^2}{r^2} + \frac{l^2}{r^2} - \frac{\left(4\zeta Q\sqrt{Q}\right)\log(r)}{3r}. \tag{8}$$

In this case, Q represents a BH's charge, and m is its mass. When ζ approaches zero, the BH becomes a RN-BH. If Q is zero, it becomes a Schwarzschild BH.

3. Equilibrium thermodynamics

In this particular segment, we shall explore equilibrium thermodynamic potentials, specifically focusing on the usual entropy of an AdS BH with NLED parameter ζ [87]. The equilibrium quantities under consideration encompass the geometric mass, Hawking temperature, and usual specific heat.

The given expression represents the geometrical mass of the BH under consideration,

$$m = \frac{l^2}{2r_h} + \frac{1}{3}(-2)\zeta Q^{3/2}\log\left(r_h\right) + \frac{Q^2}{2r_h} + \frac{r_h}{2}, \tag{9}$$

where r_h is the BH horizon radius, which is obtained by largest positive root of $h(r) = 0$. In Fig. 1 we draw hr in terms of r to find its root. We can see depend on model parameters, there are several situations. We can find a black hole with two horizons are possible as well as a naked singularity (see green dotted lines of Fig. 1). The extremal case (where two horizons coincide) is also possible which is illustrated by solid red lines of Fig. 1.

The determination of the total mass of BH can be achieved by employing the definition of mass proposed by Abbott and Deser [88,89],

$$M = \frac{m}{8} = \frac{1}{8}\Big(\frac{l^2}{2r_h} + \frac{1}{3}(-2)\zeta Q^{3/2}\log\left(r_h\right) + \frac{Q^2}{2r_h} + \frac{r_h}{2}\Big). \tag{10}$$

One of the fundamental thermodynamic potentials of great significance is the entropy associated with a BH, which can be expressed as

$$S_0 = \frac{A}{4} = \pi r_h^2. \tag{11}$$

The volumetric thermodynamic potential of the BH is expressed as

$$V = \frac{4\pi r_h^3}{3}. \tag{12}$$

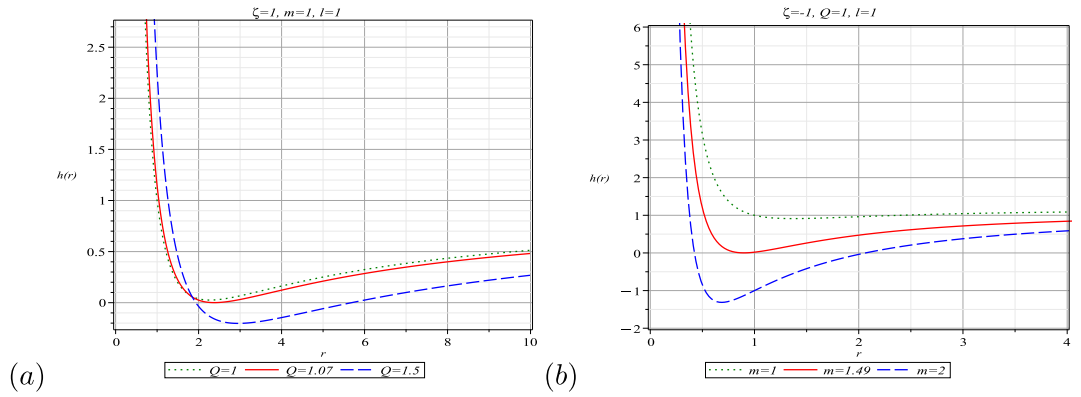

Fig. 1. Horizon structure analysis for $l = 1$. (a) we take $\zeta = 1$, $m = 1$ and vary Q. (b) we take $\zeta = -1$, $Q = 1$ and vary m. (For interpretation of the references to color in this figure legend, the reader is referred to the web version of this article.)

The Hawking temperature of the given BH is the following:

$$T = \left(-\frac{l^2}{4\pi r_h^3} - \frac{\zeta Q^{3/2}}{3\pi r_h^2} - \frac{Q^2}{4\pi r_h^3} + \frac{1}{4\pi r_h}\right). \tag{13}$$

The expression for the associated heat capacity $C = T(\frac{\partial S_0}{\partial T})$ can be represented

$$C = \frac{2\pi r_h^2\left(4\zeta Q^{3/2} r_h - 3r_h^2 + 3\left(l^2 + Q^2\right)\right)}{-8\zeta Q^{3/2} r_h + 3r_h^2 - 9\left(l^2 + Q^2\right)}. \tag{14}$$

To observe the Hawking temperature concerning the altered values of the electric charge Q and the NLED parameter ζ, we have graphically represented the Hawking temperature in Fig. 2 (left two plots). Upon careful observation, it is apparent that the values of Q and ζ, the Hawking temperature, exhibit fascinating behavior. It initially experiences a growth phase, reaching its maximum value, after which it commences a gradual decline towards its equilibrium position. Similarly, the graphical representation of specific heat is illustrated in Fig. 2 (right two plots) to observe the local stability of the system. The specific heat exhibits discontinuities at specific points, indicating a phase change between regions of stability and instability for the BH under consideration. Hence, there is the second order phase transition in this case. It means that the black hole is initially in the instable phase, then goes to the stable phase as its size decreased due to the hawking radiation. However at this point we should consider quantum effects to find real phase of this stage. It will be subjects of the next sections.

4. Corrected thermodynamical quantities due to logarithmic corrected entropy

In this particular section, we will examine the potential impacts of quantum fluctuations on the RN-BH that are associated with NLED [86]. The concept of entropy is closely connected to the horizon radius of a BH [4,90], which is of great importance in understanding the thermodynamic properties of a system. Now, we are focusing on the modified entropy that string theory and loop quantum gravity produce as a result of counting microstates. The perturbed simple logarithmic corrected entropy S_p [29,35,37,45,47,59] can be represented as

$$S_p = S_0 - \frac{1}{2}\ln(S_0 T^2), \tag{15}$$

where S_0 be zeroth order entropy. The corrected entropy of a BH can be rewritten by introducing a parameter ψ to replace the factor $\frac{1}{2}$. This substitution, whic is originally did by [36], enhances the corrected terms [58] in the expression,

$$S_p = S_0 - \psi \log\left(S_0 T^2\right). \tag{16}$$

This paper examines the thermodynamic characteristics by incorporating simple logarithmic corrections. From Eqs. (11), (13), and (16), we can write

$$S_p = \pi r_h^2 + \psi \log\left(144\pi r_h^4\right) - 2\psi \log\left(4\zeta Q^{3/2} r_h - 3r_h^2 + 3l^2 + 3Q^2\right). \tag{17}$$

Fig. 3, illustrates the monotonic and smooth increase of the modified entropy, S_p, resulting from the perturbation correction. This behavior is observed across all parameters within the specified domains. The system for large-small radii BHs is positive and continuous, obeying the second law of BH thermodynamics. Similar findings have been observed in previous studies [36,45,58,59], and [91–95]. All observed trends, including equilibrium entropy and corrected entropy, are consistently positive and increasing. The usual entropy is applicable to small-sized BHs, whereas the modified entropy is more persuasive and applicable to both large

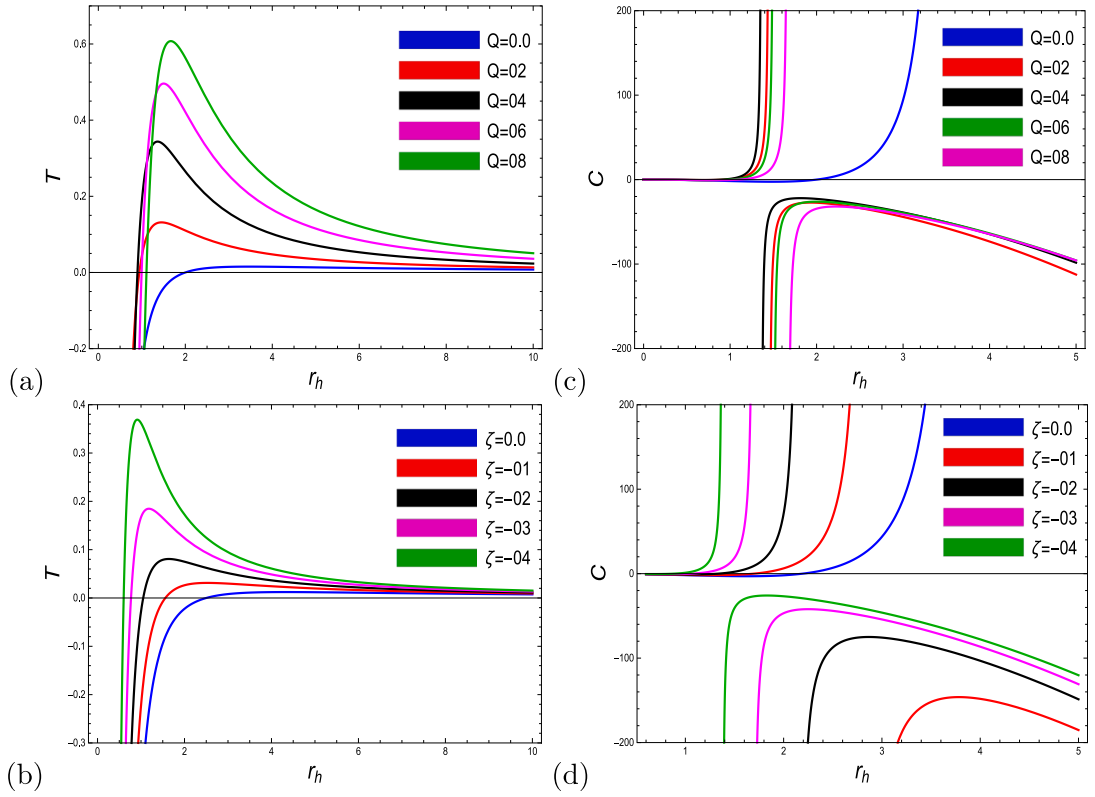

Fig. 2. The letf 2 plots indicate the graph of temperature as a function of r_h for $l = 2$. For (a) we take $\zeta = -2$, for (b) $Q = 1.50$. Similarly the right 2 plots express the graph of heat capacity as a function of r_h for $l = 2$ and for (c) we take $\zeta = -1.50$, for (d) $Q = 0.90$.

and small-sized BHs. In Ref. [58], we examined the corrected entropy of the system and found that it exhibited a positive and stable trend within the specified range. In the literature [59], we investigated the perturbed correction in entropy caused by thermal fluctuations and observed stability for very small BH horizon radii, specifically for the charged and correction parameters.

Thermal fluctuations, resulting from statistical perturbations, significantly impact small BHs, as demonstrated in Fig. 3, specifically in plots *(a)*, *(b)*, and *(c)*. It is important to note that modifying the charge parameter Q alters its behavior, causing a shift from the negative to the positive region at small horizon radii. Additionally, the plot *(a)*, demonstrates a positive, increasing trend for large radii. When the charge parameter decreases, the corrected entropy of the system increases at a faster rate. The maximum entropy of the system occurs when the charge parameter is equal to zero ($Q = 0$). This study investigates the impact of thermal fluctuations on entropy. It is found that the corrected entropy is consistently greater than the usual entropy, which is observed when the correction parameter ψ is equal to zero. The maximum corrected entropy is obtained when $\psi = 4$. Additionally, the equilibrium entropy of the BH under consideration remains stable [96]. It is worth mentioning that the thermodynamics of large BHs is not significantly influenced by small thermal fluctuations [91,93].

The Helmholtz free energy [36,45,58,59] can be modified as,

$$F_p = -\int S_p dT = -\int (S_0 - \psi \log(S_0 T^2)) dT. \tag{18}$$

Using Eqs. (11), and (17) in Eq. (18), we obtain the form of Helmholtz free energy as following,

$$\begin{aligned} F_p = \frac{-1}{12\pi r_h^3}\Big(&-9\pi r_h^2(l^2+Q^2) + \psi \log(144\pi r_h^4)(-4\zeta Q^{3/2} r_h + 3r_h^2 - 3(l^2+Q^2)) + 2\psi(4\zeta Q^{3/2} r_h \\ &-3r_h^2 + 3(l^2+Q^2))\log(4\zeta Q^{3/2} r_h - 3r_h^2 + 3(l^2+Q^2)) - 4\zeta Q^{3/2}\psi r_h + 8\pi\zeta Q^{3/2} r_h^3 \log(r_h) - 3\pi r_h^4 \\ &-4\psi(l^2+Q^2)\Big). \end{aligned} \tag{19}$$

Fig. 4 illustrates the interpretation of the perturbed corrected Helmholtz free energy F_p, for the AdS charged BH with a NLED parameter. The free energy graph demonstrate distinct behaviors, such as stability and instability, exhibited by various parameters as their domains increase. Some articles, [36,45,55,56,58,59,91,93,95–98] discussed the observation of modified Helmholtz free energy. The Helmholtz free energy, as discussed in [58], exhibits a consistent, positive, and stable trend across all parameters and domains under consideration. In our literary analysis [59], we observed a phase transition from an unstable region to a stable

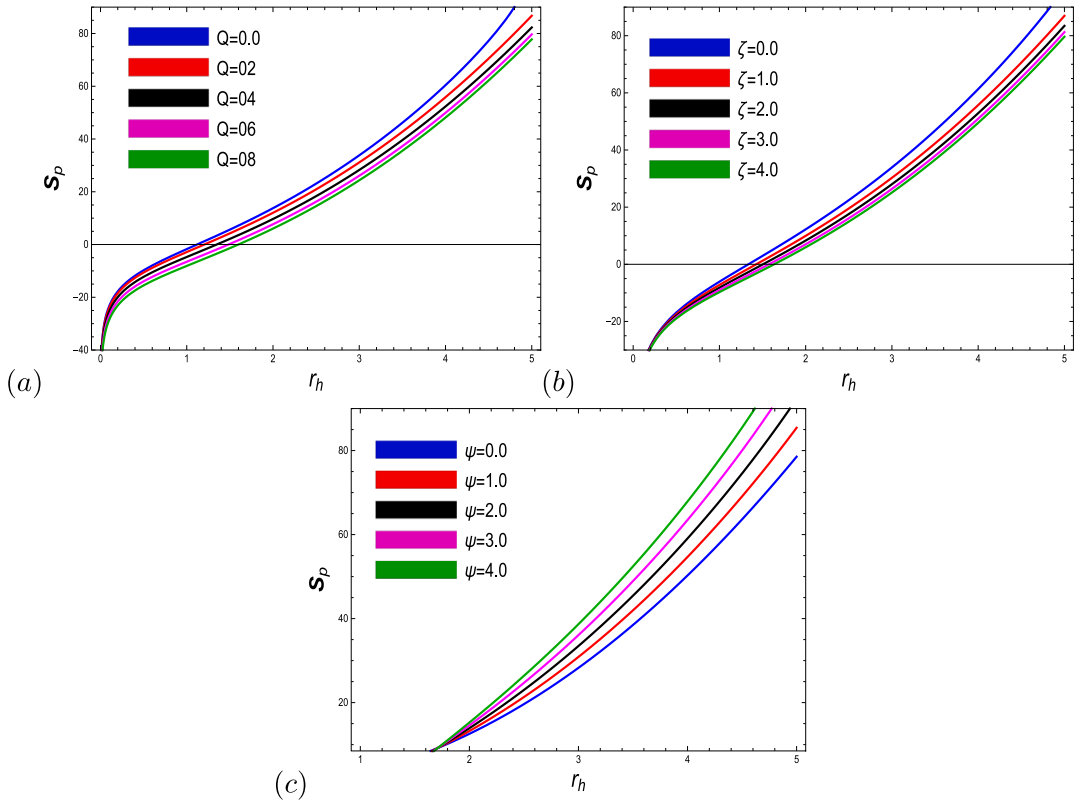

Fig. 3. This figure illustrates the graph of logarithmic corrected entropy as a function of r_h for a specific value of $l = 5$ and for plot (a), we take $\zeta = 1$, $\lambda = 2$, for (b), $Q = 3$, $\lambda = 3$ and for (c), $Q = 4$, $\zeta = 0.2$.

region, followed by a progression towards equilibrium for charged and correction parameters. In Fig. 4 plot*(a)*, it is evident that as the charge parameter increases, the Helmholtz free energy undergoes a phase transition from an unstable state to a stable state and then returns to an unstable state for the specific range of charge values from $Q = 02$ to $Q = 08$. The Helmholtz free energy is stable for all considered domains when $Q = 0$ (blue line). When examining the stable region, it is observed that the Helmholtz free energy reaches its maximum value at a charge parameter of $Q = 8$ (indicated by the green line). As the parametric values increase, the Helmholtz free energy in the domain system also increases, reaching its highest value. The modified Helmholtz free energy is depicted in plot *(b)*, both with and without the inclusion of the NLED parameter ζ. The energy remains negative across the critical horizon radii. The critical horizon radius is the point at which thermal fluctuations, whether perturbed or non-perturbed, have no effect on the Helmholtz free energy. It is observed that the Helmholtz free energy undergoes a phase transition in its phase space, transition from negative to positive and then from positive to negative, when the non-zero NLED parameter ζ is considered. In the absence of the coupling parameter $\zeta = 0$ (blue line), the Helmholtz free energy function remains stable across the entire range of the horizon radius. The graphical profile in plot *(c)*, shows the relationship between the Helmholtz free energy and the correction parameter ψ. It indicates that the energy becomes stable after transition from an unstable region. The free energy initially increases to its maximum value and then gradually decreases in all the regions under consideration. Therefore, we can infer that the system is stable, indicating that it absorbs a greater amount of energy from its surroundings. With correction parameter due to thermal fluctuations, the energy is higher for both small and large BH radii. Therefore, it can be inferred that the inclusion of logarithmic correction results in an increase in the Helmholtz free energy rather than the energy without correction. Additionally, the presence of a logarithmic correction leads to a decrease in the stability of charged AdSBH with NLED. The free energy system remains stable across all domains. Several articles [36,91,96] have reported results showing a decrease in the Helmholtz free energy as a result of fluctuations.

Now, we can proceed to calculate the total corrected mass [58,59,99], by utilizing the concept of a thermodynamic system,

$$\tilde{M}_p = F_p + S_p T = F_p + (S_0 - \psi \log(S_0 T^2))T, \tag{20}$$

Using Eqs. (11), (17), and (19) in Eq. (20), we find,

$$\tilde{M}_p = \left(\frac{l^2\psi}{3\pi r_h^3} + \frac{l^2}{2r_h} + \frac{\zeta Q^{3/2}\psi}{3\pi r_h^2} - \frac{2}{3}\zeta Q^{3/2}\log(r_h) + \frac{Q^2\psi}{3\pi r_h^3} + \frac{Q^2}{2r_h} + \frac{r_h}{2} - \frac{1}{3}\zeta Q^{3/2}\right). \tag{21}$$

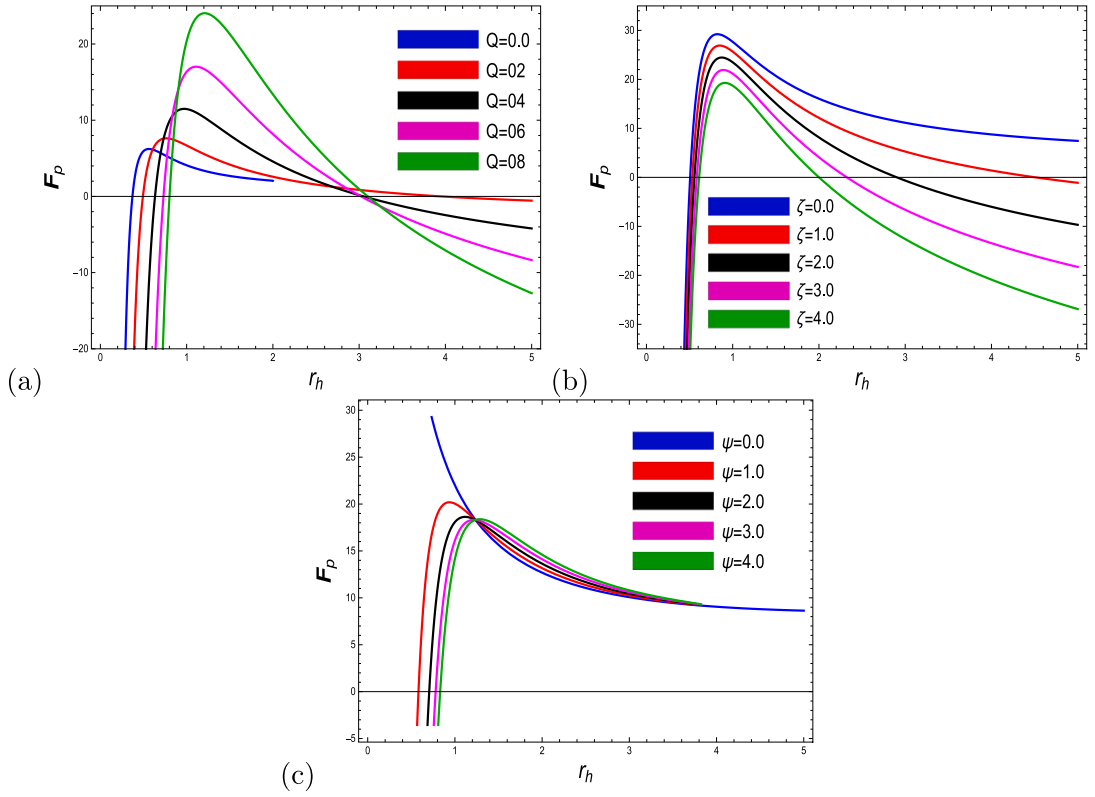

Fig. 4. This figure illustrates the graph of logarithmic corrected Helmholtz free energy as a function of r_h for a specific value of $l = 5$ and for plot (a), we take $\zeta = 1$, $\lambda = 1$, for (b), $Q = 4$, $\lambda = 0.50$ and for (c), $Q = 2$, $\zeta = -1$. (For interpretation of the references to color in this figure legend, the reader is referred to the web version of this article.)

Fig. 5, illustrates the relationship between the total modified mass $\tilde{M}_p$ and BH radius. The total corrected mass exhibits an initially descending trend, reaching a minimum value, and then showing an ascending pattern as all given parameters increase. The literature [58,59,91,98,99], presents similar findings, suggesting that the physical masses of the BHs being studied consistently increase from their minimal value to reach their maximal. The stability of all three parameters was observed to increase as the horizon radii values increased, as stated in Ref. [58]. Additionally, the maximum corrected mass values can be achieved by using the highest values for each of the three parameters. The total corrected mass exhibits an endothermic process, indicating that it absorbs energy from its surroundings. The maximum value of the total corrected mass occurs when the correction parameter is at its smallest value, which is $\eta = 1$. From Fig. 5, plot *(a)*, it has been shown that as charge parameter Q increases, mass stays constant at higher charge parameter values. At first, the corrected mass system begins to progressively decline toward equilibrium. According to the green line, the provided domain has its highest energy at $Q = 8$. The plot *(b)*, illustrates the impact of the NLED parameter ζ. The $\zeta = 0$, recovers the complete corrected mass, as shown by the RN-BH [58,100]. It is discovered that for large radii, the physical mass grows in both circumstances (with and without the presence of NLED). Furthermore, the existence of the NLED parameter reduces the internal energy of the system compared to the absence of the NLED parameter. We show the total physical mass with and without modification in the plot *(c)*. The energy of the system can initially drop to a minimum and then begin to rise for large radii.

The necessity for the first law to remain valid for BH thermodynamical quantities in the presence of thermal fluctuations leads to the formulation of a modified first law of BH thermodynamics,

$$\tilde{M} = \tilde{T}\delta S + \phi\delta Q + \tilde{V}\delta P = 0, \tag{22}$$

The variables $\tilde{T}$, ϕ, and $\tilde{V}$ are used to represent the corrected temperature, electric potential, and corrected volume, respectively. The identification of modified thermodynamic characteristics can be achieved by utilizing the following expressions,

$$\tilde{T} = (\frac{\partial \tilde{M}}{\partial S})_Q$$

$$\phi = (\frac{\partial \tilde{M}}{\partial Q})_S$$

$$\tilde{V} = (\frac{\partial \tilde{M}}{\partial P})_{S,Q}$$

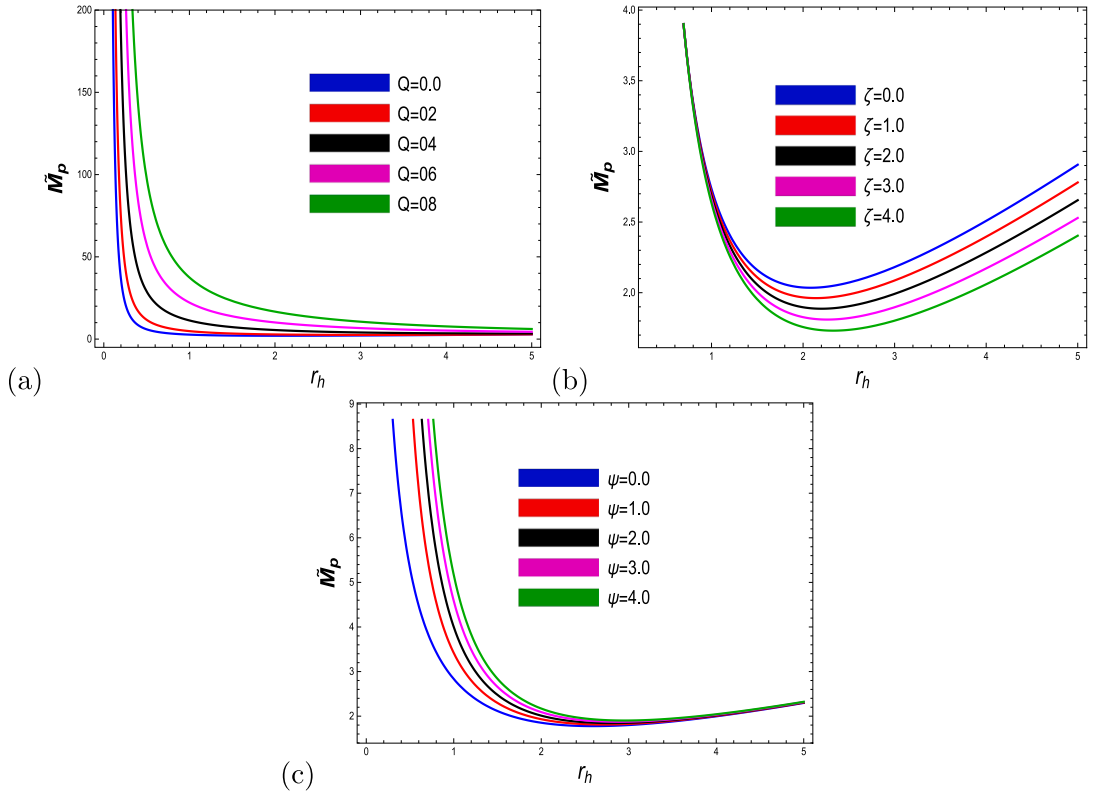

Fig. 5. This figure illustrates the graph of logarithmic corrected total mass as a function of r_h for a specific value of $l = 5$ and for plot (a), we take $\zeta = 0.10$, $\lambda = 0.50$, for (b), $Q = 0.20$, $\lambda = 0.50$ and for (c), $Q = 1$, $\zeta = 0.50$. (For interpretation of the references to color in this figure legend, the reader is referred to the web version of this article.)

which gives

$$\tilde{T} = \left(-\frac{l^2}{4\pi r_h^3} - \frac{\zeta Q^{3/2}}{3\pi r_h^2} - \frac{Q^2}{4\pi r_h^3} + \frac{1}{4\pi r_h}\right). \tag{23}$$

The corresponding perturbed corrected pressure [36,45,55,58,59] of the AdS charged BH with an NLED are given by

$$P_p = -\frac{dF_p}{dV}, \tag{24}$$

which is yields to the following expression,

$$P_p = \frac{1}{48\pi^2 r_h^6}\Big((8\zeta Q^{3/2} r_h - 3r_h^2 + 9(l^2+Q^2))(\psi(\log(144\pi r_h^4) - 2\log(4\zeta Q^{3/2} r_h - 3r_h^2 + 3(l^2+Q^2))) + \pi r_h^2)\Big). \tag{25}$$

The modified pressure has been reported in previous studies [36,45,55,58,59,93,96,101]. The articles [36,45], demonstrated the correction parameter resulted in a decrease in modified pressure. The pressure, as corrected for perturbations [58], diverges from the stable region for charged and correction parameters. However, it exhibits stability after the phase transition for the coupling parameter. The pressure of a Torus-like charged BH was corrected in a study by [59]. This study investigates the phase transition that occurs as the BH transitions from an unstable state to a stable state, ultimately reaching equilibrium. Thermal fluctuations have a greater impact on small BTZ BHs [93]. The pressure of regular BHs [101], is significantly affected by logarithmic correction. The corrected pressure due to perturbed correction P_p for the horizon radius r_h is shown in Fig. 6. The pressure analysis involves three parameters: Q, ζ, and ψ. The occurrence of a second-order phase transition can be observed when varying the charge parameter, coupling parameter, and corrected parameter, as the system transitions from an unstable state to a stable state and eventually reaches an equilibrium state. The plot *(a)*, initially take transitions from a negative phase to a positive phase and then stabilizes at an equilibrium state. At a value of $Q = 8$, the system achieves its maximum corrected pressure. Similar occurrences can be observed in plots *(b)* and *(c)*. It is crucial to note from plots *(b)* and *(c)* that during the initial increasing phase, the maximum pressure values occur at $\zeta = 0$ and $\psi = 0$. In the subsequent phase of decreasing towards equilibrium, the highest increasing pressure is observed at $\zeta = 4$ and $\psi = 4$ across the entire domain.

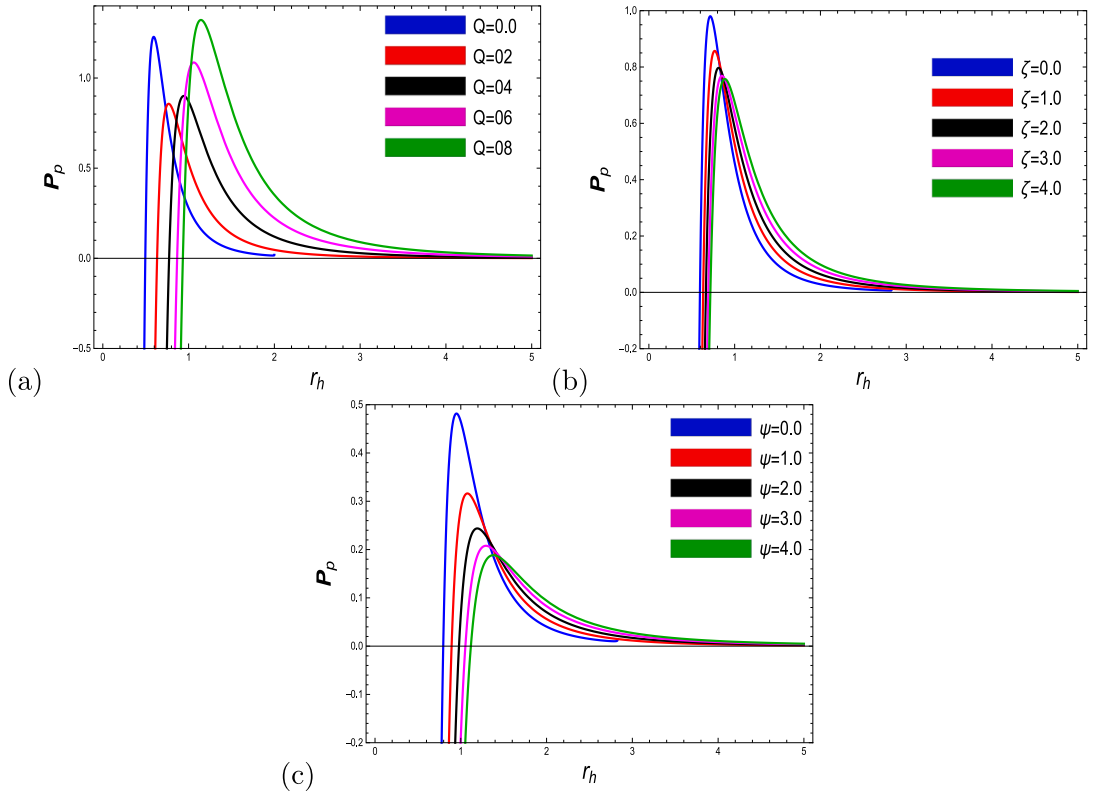

Fig. 6. This figure illustrates the graph of logarithmic corrected pressure as a function of r_h for a specific value of $l = 5$ and for plot (a), we take $\zeta = 1$, $\lambda = 0.50$, for (b), $Q = 2$, $\lambda = 0.50$ and for (c), $Q = 2$, $\zeta = 1$.

To accurately determine the perturbed corrected enthalpy H_p of a thermodynamical system [36,45,55,99],

$$H_p = \tilde{M}_p + P_p V, \tag{26}$$

$$\begin{aligned} H_p = \frac{1}{36\pi r_h^3}\Big((8\zeta Q^{3/2} r_h - 3r_h^2 + 9(l^2+Q^2))(\psi(\log(144\pi r_h^4) - 2\log(4\zeta Q^{3/2} r_h - 3r_h^2 + 3(l^2+Q^2))) \\ +\pi r_h^2) + 18\pi l^2 r_h^2 + 12\zeta Q^{3/2}\psi r_h - 12\pi\zeta Q^{3/2} r_h^3 - 24\pi\zeta Q^{3/2} r_h^3 \log(r_h) + 18\pi Q^2 r_h^2 + 18\pi r_h^4 \\ + 12 l^2\psi + 12 Q^2\psi\Big). \end{aligned} \tag{27}$$

Fig. 7, displays the graphical representation of the corrected enthalpy H_p in relation to the horizon r_h. In general, the enthalpy exhibits a positive and increasing trend for larger BH radii, denoted as r_h. Previous research has examined the system's enthalpy, specifically in relation to thermal fluctuations, in several studies [36,55,56,58,59,93,96]. The enthalpy of the system is more appropriate for large radius BHs when considering the correction parameter [56]. The corrected enthalpy, as examined in [58], assessed the stability of all three parameters across the entire domain. The enthalpy of the system decreased from a stable state to an equilibrium state due to the charged parameter. Similarly, the correction parameter increased from a lower region to an equilibrium state, as observed in [59]. The enthalpy of the system characterizes the phase transition from an unstable to a stable region across all parameters. The enthalpy rises to its peak for small radii, providing stability across the entire domain for all values of the charged parameter in plot *(a)*. The maximum value of corrected enthalpy across the entire domain occurs at $Q = 8$. Plot *(b)*, exhibits comparable behavior, with the exception that the maximum enthalpy value is associated with the absence of the NLED parameter ζ. Therefore, the system can achieve its maximum enthalpy without the need for NLED. Enthalpy is observed to be associated with increased stability in the presence of the NLED parameter. In plot *(c)*, the graph demonstrates an increasing trend for the given radii when the value of Q is fixed and the parameter ψ is corrected. The presence of a correction parameter leads to the occurrence of phase space transitions from instability to stability, followed by a gradual decrease for specific radii and then an increase for larger radii.

The investigation of global stability necessitates the definition of the Gibbs free energy [36,55,56,58,59,93,96],

$$G_p = H_p - TS_p = H_p - T(S_0 - \psi\log(S_0 T^2)). \tag{28}$$

The Gibbs free energy can be expressed in the following manner, based on the quantities indicated above:

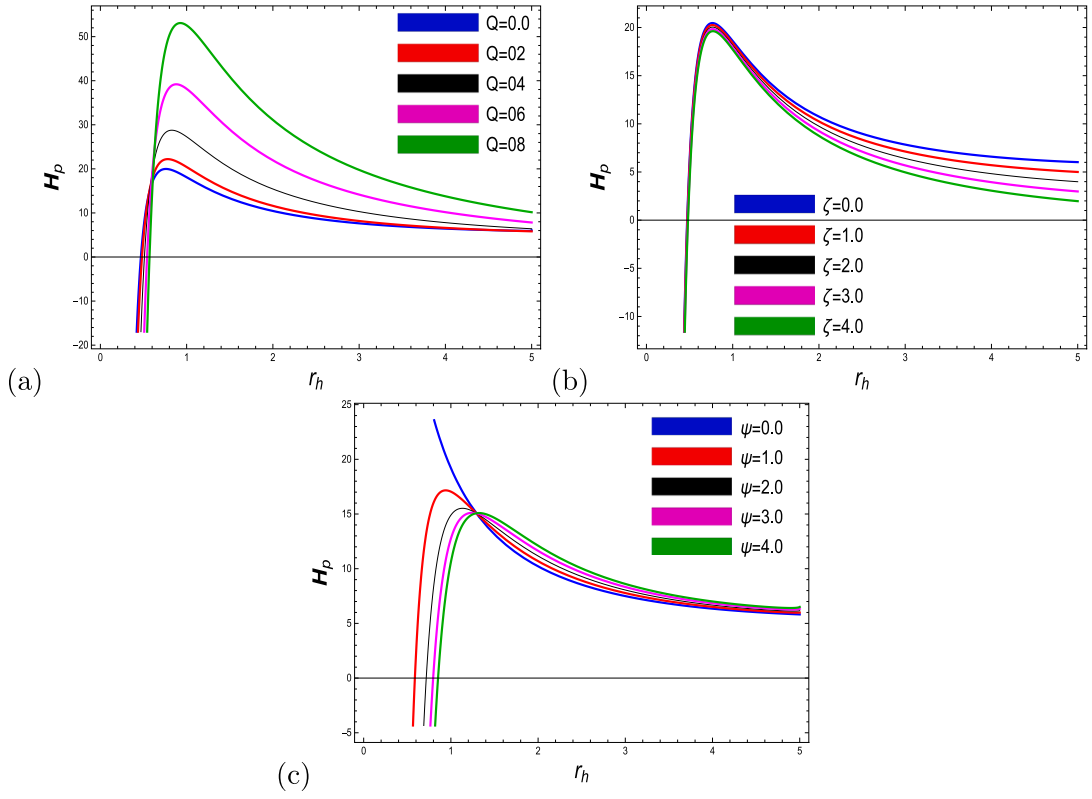

Fig. 7. This figure illustrates the graph of logarithmic corrected enthalpy as a function of r_h for a specific value of $l = 5$ and for plot (a), we take $\zeta = 0.20$, $\lambda = 0.50$, for (b), $Q = 0.90$, $\lambda = 0.50$ and for (c), $Q = 0.20$, $\zeta = 0.20$.

$$G_p = \frac{1}{18\pi r_h^3}\Big(3\psi(l^2+Q^2)(-6\log(4\zeta Q^{3/2}r_h - 3r_h^2 + 3(l^2+Q^2)) + 3\log(144\pi r_h^4) + 2) + r_h (2\zeta Q^{3/2}\psi(-10\log(4\zeta Q^{3/2}r_h - 3r_h^2 + 3(l^2+Q^2)) + 5\log(144\pi r_h^4) + 3) + r_h(6(2\psi\log(4\zeta Q^{3/2}r_h - 3r_h^2 + 3(l^2+Q^2)) - \psi\log(144\pi r_h^4) + 3\pi(l^2+Q^2)) + \pi r_h(4\zeta Q^{3/2}(1 - 3\log(r_h)) + 3r_h)))\Big). \tag{29}$$

Fig. 8, illustrates the relationship between Gibbs free energy and BH radius, highlighting the importance of all three parameters. Numerous articles in the literature discuss the Gibbs free energy [36,45,58,59,91,92,95]. Pourhassan [36], observed that the involvement of thermal fluctuations leads to a decrease in the Gibbs free energy of the BH system. Abbas [58], explored that the given system of Gibss free energy remains increasing and stable for the considered domain. Abbas [59], also investigated the second-order phase transition in order to measure the Gibss free energy associated with charged and correction parameters and conclude that Gibss free energy reaches equilibrium from the negative region. The physical profile of the Gibbs free energy in [91,92], demonstrates that thermal fluctuation effects only small BHs. The behavior of Gibss free energy is similar to the corrected enthalpy of the system, which was discussed in detail earlier.

The concept of specific heat [45,58], is employed to analyze the local stability of the BH. The modified heat capacity $C_p = \frac{TdS_p}{dT}$ can be expressed as

$$C_p = -\frac{2\left(r_h\left(\pi r_h\left(4\zeta Q^{3/2}r_h - 3r_h^2 + 3\left(l^2+Q^2\right)\right) + 4\zeta Q^{3/2}\psi\right) + 6\psi\left(l^2+Q^2\right)\right)}{8\zeta Q^{3/2}r_h - 3r_h^2 + 9\left(l^2+Q^2\right)}. \tag{30}$$

As far as concern to Fig. 9, which illustrates the physical interpretation of heat capacity due to perturbation correction $C_p = 0$ in terms of r_h. Numerous studies, such as [36,45,55,56,58,91,96,99], have examined heat capacity under quantum fluctuations. The article [96], states that heat capacity is unstable without logarithmic correction but becomes stable for small BH with the presence of thermal fluctuations. In Fig. 9, the plot *(a)*, which reveals that phase shifts exclusively for low values of the charge parameter. Specific heat undergoes a phase shift from instability to stability between the values $Q = 0$ and $Q = 2$. The specific heat regarding charged parametric values from $Q = 4$, to $Q = 8$ remain unstable. From plot *(b)*, exhibit that in initial phase specific heat converges from instability to stability state. It may noted that for large sized BH the associated specific heat becomes more stable as the values

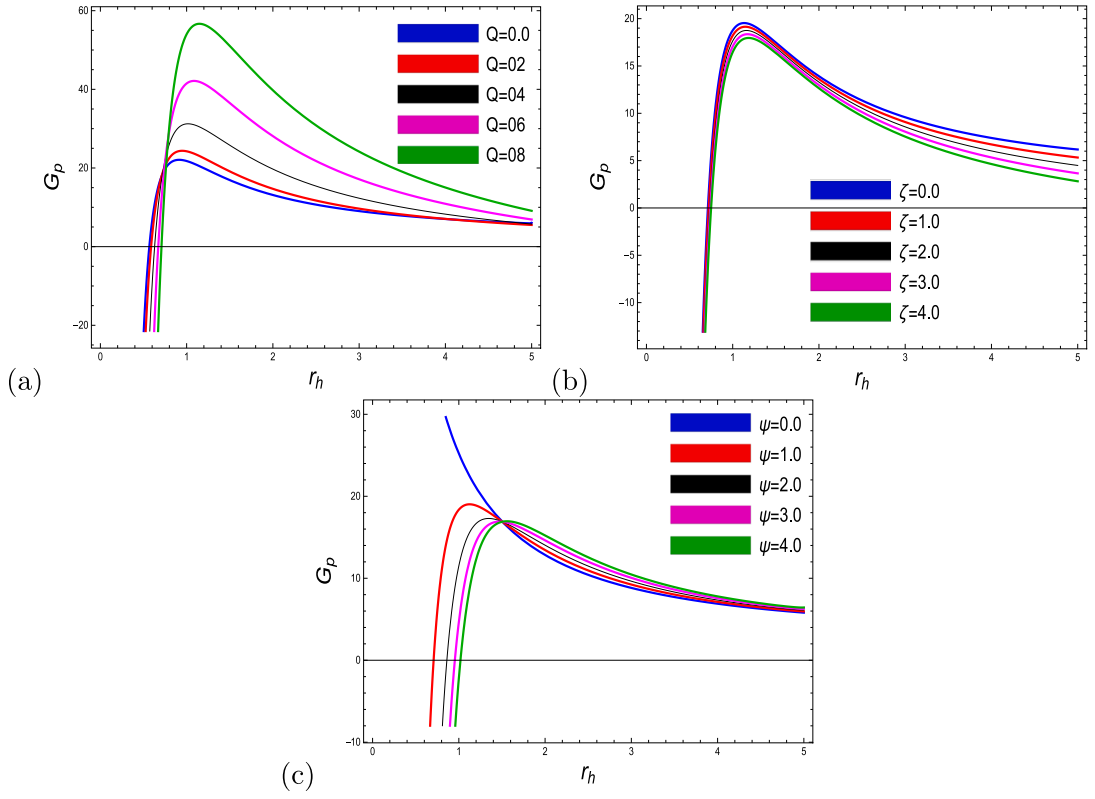

Fig. 8. This figure illustrates the graph of logarithmic corrected Gibbs free energy as a function of r_h for a specific value of $l = 5$ and for plot (a), we take $\zeta = 0.50$, $\lambda = 0.50$, for (b), $Q = 1$, $\lambda = 1$ and for (c), $Q = 0.20$, $\zeta = 0.50$.

of the NLED parameter decrease. To check the impact of the existence of the logarithmic correction due to thermal fluctuation, we focus our attention on plot *(c)*, which describes the occurrence of the phase transition and how specific heat is convergent from the unstable to the stable region.

5. Corrected thermodynamical quantities due to exponential corrected entropy

In the main section of this paper, we aim to investigate the non-perturbed (exponential) correction regarding the entropy of a considered BH. According to what we found, the entropy of a BH has an exponential correction when counting microstates, which is done only for quantum states. This means that the exponential correction term is important when thinking about BHs with smaller surface areas, which have big quantum effects at short distances [15]. The exponential correction is given by [61],

$$S_{np} = S_0 + \lambda \exp(-S_0), \tag{31}$$

where λ, be the correction parameter [102,103]. Using the Eq. (11), we get

$$S_{np} = \lambda \exp\left(-\pi r_h^2\right) + \pi r_h^2. \tag{32}$$

We observe that Fig. 10, serves as a visual representation depicting the physical profile of exponentially corrected entropy S_{np}, with respect to the horizon radius r_h. The entropy of a given BH undergoes a reduction in size as a consequence of the existence of non-perturbed corrections characterized by diverse values of the correction parameter λ. To ensure we uphold the second law of thermodynamics, we focus on utilizing positive values of the correction parameter, $\lambda > 0$. The observed patterns of the corrected entropy in the regime of reduced r_h the profound influence of quantum corrections, as evidenced by the fluctuations at this particular scale, which are contingent upon the exponential correction parameter λ. The entropy that usually occurs when $\lambda = 0$, is depicted by the blue line, which exhibits a restoration of the conventional Bekenstein–Hawking entropy relation. Furthermore, it is worth noting that the corrected entropy of the entire system reaches its highest value at $\lambda = 4$, and its lowest value at $\lambda = 0$.

The Helmholtz free energy, as described by the exponentially corrected formulation [68], can be expressed in the following manner:

$$F_{np} = -\int S_{np} dT = -\int (S_0 + \lambda \exp(-S_0)) dT. \tag{33}$$

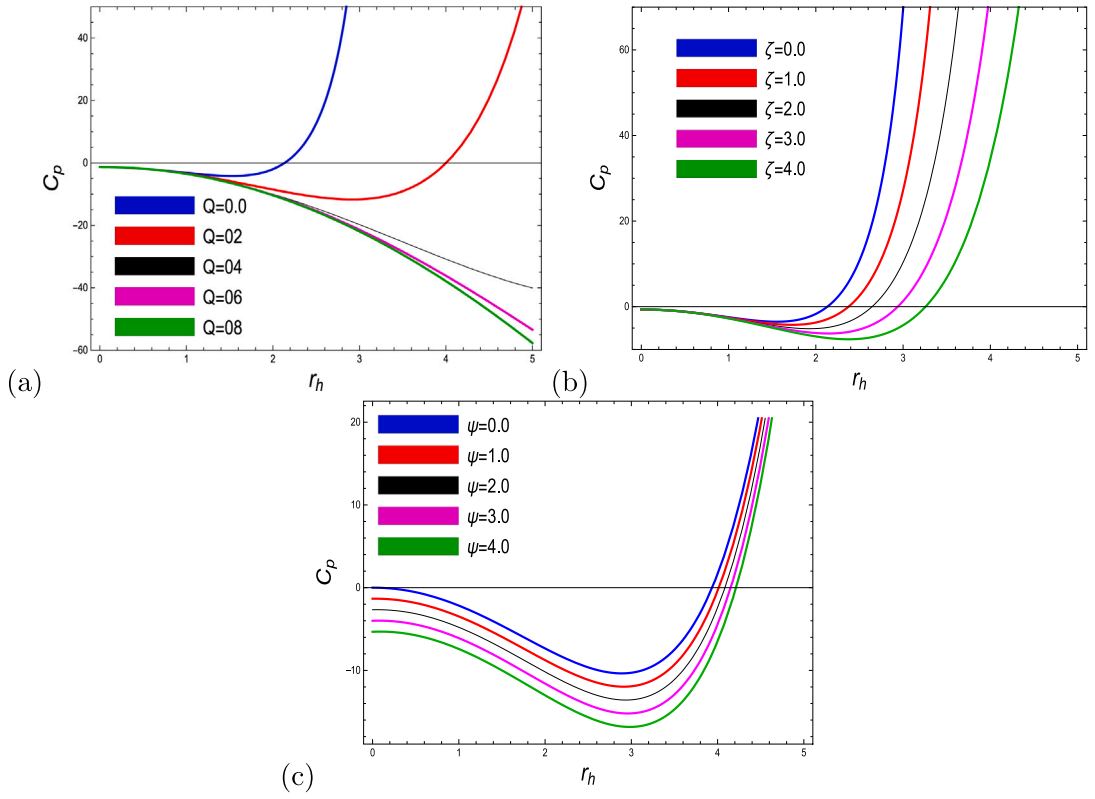

Fig. 9. This figure illustrates the graph of logarithmic corrected specific heat as a function of r_h for a specific value of $l = 5$ and for plot (a), we take $\zeta = 0.50$, $\lambda = 1$, for (b), $Q = 0.50$, $\lambda = 0.50$ and for (c), $Q = 1$, $\zeta = 2$.

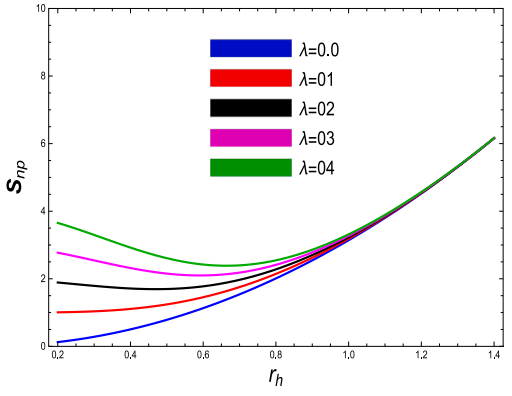

Fig. 10. The given figure express the graph of corrected entropy as a function of r_h. (For interpretation of the references to color in this figure legend, the reader is referred to the web version of this article.)

Using Eqs. (11), (13), and (33), we get the form of Helmholtz free energy:

$$F_{np} = \frac{-1}{12\pi}\Big(3\pi\lambda\left(2\pi l^2 + 2\pi Q^2 + 1\right)\mathrm{erf}\left(\sqrt{\pi}r_h\right) - 4\pi\zeta\lambda Q^{3/2}\mathrm{Ei}\left(-\pi r_h^2\right) + 8\pi\zeta Q^{3/2}\log\left(r_h\right) - 3\pi r_h$$
$$- \frac{1}{r_h}9\pi\left(l^2 + Q^2\right) + \frac{\lambda\exp\left(-\pi r_h^2\right)\left(r_h^2\left(6\pi l^2 + 6\pi Q^2 + 3\right) - 4\zeta Q^{3/2} r_h - 3\left(l^2 + Q^2\right)\right)}{r_h^3}\Big). \tag{34}$$

The exponentially corrected Helmholtz free energy function F_{np} of RN-BH, coupled with the NLED parameter associated with the horizon radius r_h, appears as captivating graphical features in Fig. 11. It is observed that the stability of the Helmholtz free energy

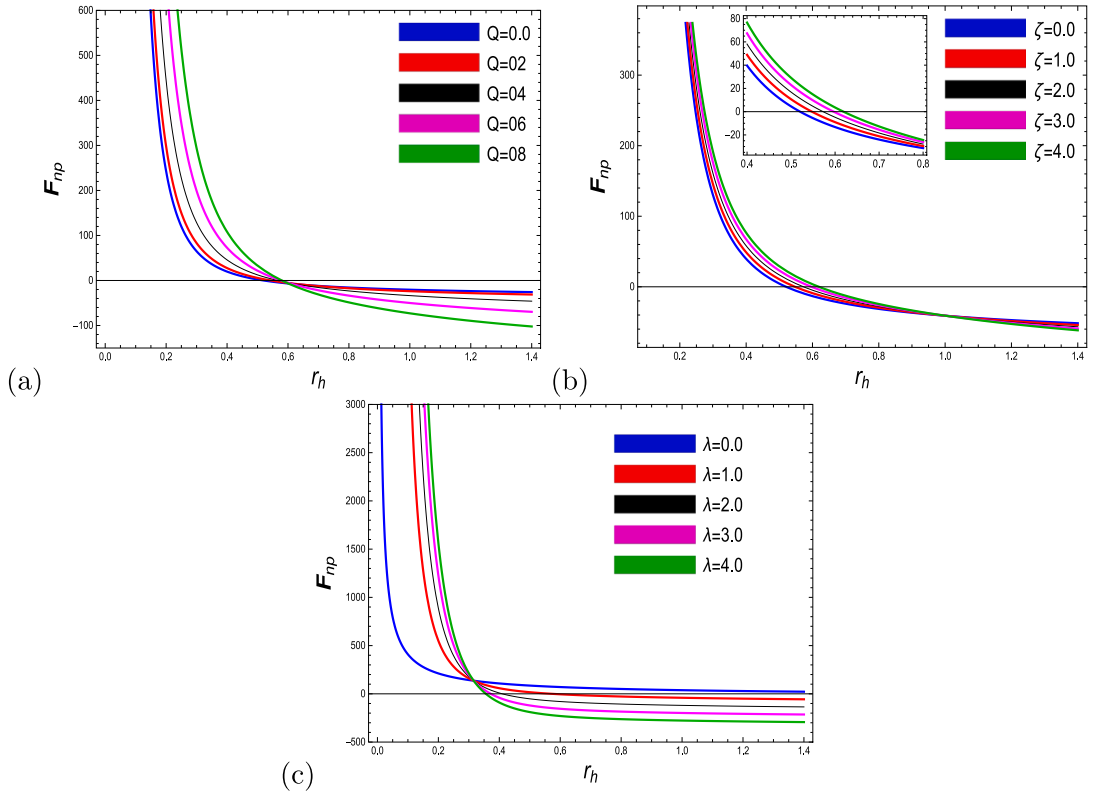

Fig. 11. The figure illustrates the graph of Helmholtz free energy as a function of r_h for a specific value of $l = 5$ and for plot (a), we take $\zeta = 2$, $\lambda = 1$, for (b), $Q = 5$, $\lambda = 1$ and for (c), $Q = 2$, $\zeta = 2$..

is limited to small radii for all three plots, specifically when $r_h < 0.8$. This observation holds true for all three parameters, namely the charged parameter Q, the coupling parameter ζ, and the non-perturbed exponentially corrected parameter λ. The Helmholtz free energy exhibits a decrease as the horizon radius increases while simultaneously diverging from the stable to the unstable region across all parameters. It is duly observed that the Helmholtz free energy attains its maximum state when all three parameters reach their maximum values, while the Helmholtz free energy reaches its lowest state when $Q = 0$, $\zeta = 0$, and $\lambda = 0$ respectively.

The total corrected mass can be estimated as,

$$\tilde{M}_{np} = F_{np} + S_{np}T = F_{np} + (S_0 + \lambda \exp(-S_0))T, \tag{35}$$

Using Eqs. (11), (13) and (34) in Eq. (35), one can get the required corrected mass as,

$$\tilde{M}_{np} = \frac{1}{12r_h}\Big(\exp(-\pi r_h^2)(\exp(\pi r_h^2)(r_h(-3\lambda(2\pi(l^2+Q^2)+1)\mathrm{erf}(\sqrt{\pi}r_h) + 4\zeta Q^{3/2}(\lambda \mathrm{Ei}(-\pi r_h^2) - 2\log(r_h) - 1) + 6r_h) + 6(l^2+Q^2)) - 6\lambda(l^2+Q^2))\Big). \tag{36}$$

The pressure of the considered BH with NLED can be determined as,

$$P_{np} = -\frac{dF_{np}}{dV}, \tag{37}$$

From above mentioned equations, we have

$$P_{np} = \frac{1}{48\pi^2 r_h^6}\Big(\exp\left(-\pi r_h^2\right)\left(\pi r_h^2 \exp\left(-\pi r_h^2\right) + \lambda\right)\left(8\zeta Q^{3/2} r_h - 3r_h^2 + 9\left(l^2+Q^2\right)\right)\Big).$$

The exponentially corrected pressure P_{np} of a given BH is visually expressed in Fig. 12. The pressure initially exhibits a stable behavior for very small BH but gradually decreases towards an equilibrium state as the horizon radius increases. This pattern is consistently observed across all three plots. The observable consequences arising from quantum fluctuations in non-perturbations can be observed. Plots *(a)*, and *(c)*, show that the highest corrected pressure can be obtained by using the largest values of the charged parameter at $Q = 8$, as well as the non-perturbed correction parameter at $\lambda = 4$. Plot *(b)*, demonstrates the opposite trend. Therefore, the stability of a quantum BH can be analyzed by considering the exponentially corrected pressure due to quantum fluctuations, which ultimately leads to the system reaching an equilibrium state within a given domain.

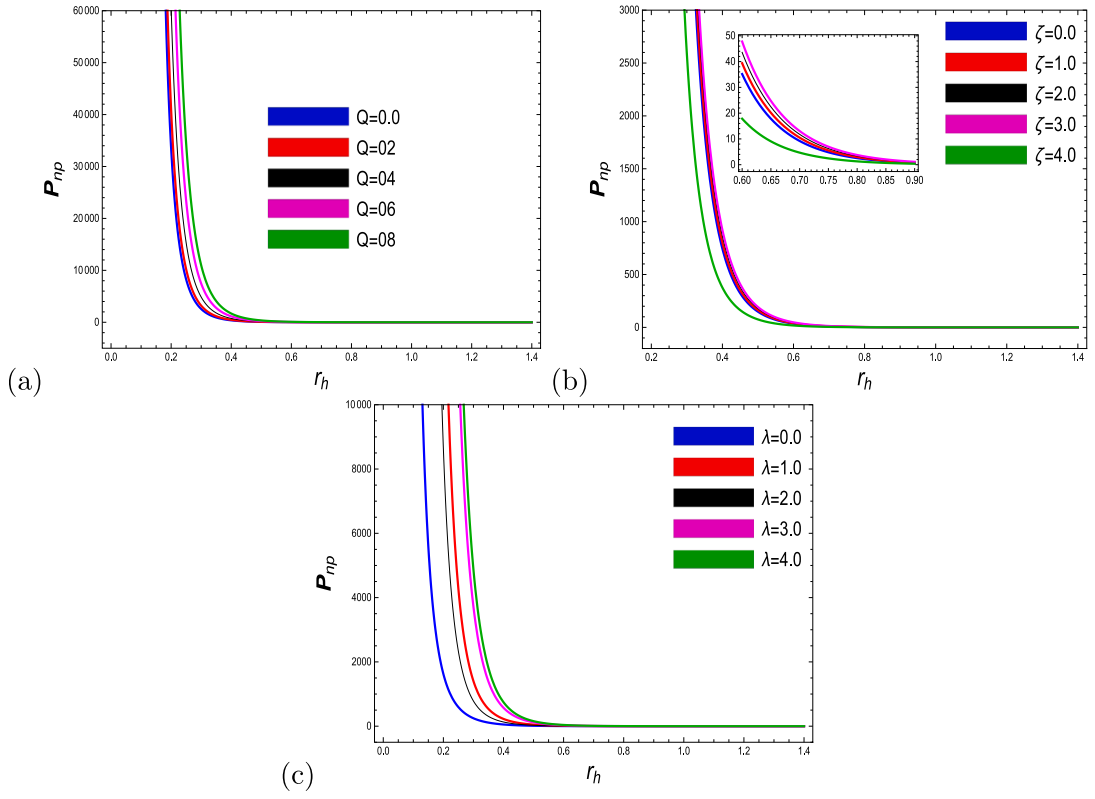

Fig. 12. This figure illustrates the graph of exponentially corrected pressure as a function of r_h for a specific value of $l = 5$ and for plot (a), we take $\zeta = 3$, $\lambda = 5$, for (b), $Q = 5$, $\lambda = 1$ and for (c), $Q = 5$, $\zeta = 3$.

The enthalpy due to the exponential correction can be estimated as

$$H_{np} = \tilde{M}_{np} + P_{np}V, \tag{38}$$

By employing the aforementioned quantities, we obtain

$$\begin{aligned} H_{np} = \frac{1}{36r_h^3}\Big(&3r_h^2(\exp(-\pi r_h^2)(r_h(-3\lambda(2\pi(l^2+Q^2)+1)\mathrm{erf}(\sqrt{\pi}r_h)+4\zeta Q^{3/2}(\lambda \mathrm{Ei}(-\pi r_h^2) \\ &-2\log(r_h)-1)+6r_h)+6(l^2+Q^2))-6\lambda(l^2+Q^2)+\exp(-\pi r_h^2))\frac{1}{\pi}((9(l^2+Q^2) \\ &+8\zeta Q^{3/2}r_h-3r_h^2)\pi r_h^2\exp(-\pi r_h^2)+\lambda)\Big). \end{aligned} \tag{39}$$

The enthalpy of the system can be positively influenced by the non-perturbed exponential correction with respect to the horizon radius r_h. Its physical profile is depicted in Fig. 13. We can explore the exciting physical behavior of corrected enthalpy by dividing it into three phases. The initial phase is stable, followed by an unstable phase, and finally, we reach the equilibrium phase in all plots for all three parameters. It is exciting to see that at the start, the enthalpy remains stable for a very small BH radius and then gradually decreases to reach its minimum before moving towards the unstable region. The phase transition will occur again, bringing stability and equilibrium to the system, especially for larger radii in the given domain. From Fig. 13, plot *(a)*, it is evident that the enthalpy associated with charged parameter reaches its maximum value with the largest value of Q, in the stable region. Similarly, it attains its minimum value with the largest value of Q, in the unstable region. The plot *(b)*, shows that with the highest value of the NLED parameter, the corresponding corrected enthalpy remains at its maximum for both stable and unstable regions. This suggests that there is potential for significant and positive outcomes in these regions. In the absence of the correction parameter $\lambda = 0$, the enthalpy of the system remains stable for all given domains, gradually approaching equilibrium. Furthermore, it is worth noting that the enthalpy reaches its highest value at $\lambda = 4$, but it remains at a minimum for both regions, from stable to unstable. Gibbs free energy is defined to investigate global stability as

$$G_{np} = H_{np} - TS_{np} = H_{np} - T(S_0 + \lambda\exp(-S_0)). \tag{40}$$

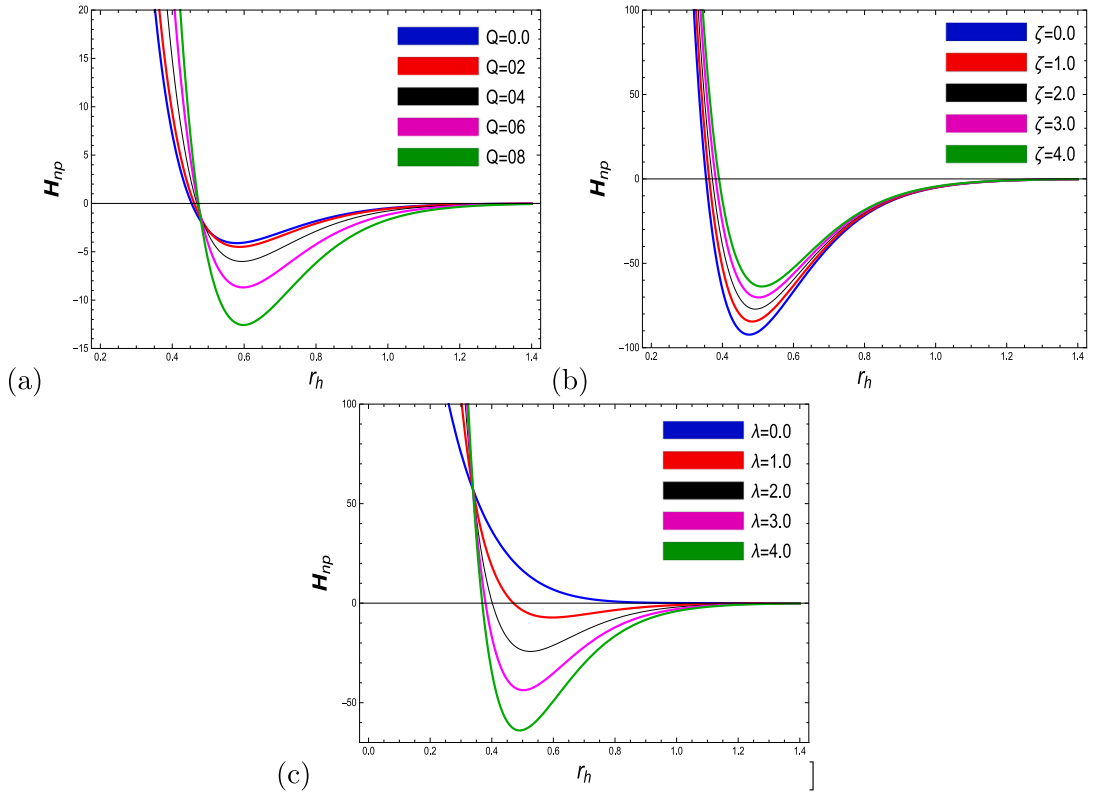

Fig. 13. This figure illustrates the graph of exponentially corrected enthalpy as a function of r_h for a specific value of $l = 5$ and for plot (a), we take $\zeta = 1$, $\lambda = 1$, for (b), $Q = 5$, $\lambda = 1$ and for (c), $Q = 5$, $\zeta = 1$.

In order to explore the global stability of a system, one must consider the concept of Gibbs free energy, which is mathematically defined as

$$G_{np} = \frac{1}{36\pi r_h^3}(\exp(-2\pi r_h^2))\Big(\pi r_h^2(r_h(-9\lambda(2\pi(l^2+Q^2)+1)\mathrm{erf}(\sqrt{\pi}r_h) + 4\zeta Q^{3/2}(3\lambda \mathrm{Ei}(-\pi r_h^2) \\ -6\log(r_h)-1)+15r_h)+27(l^2+Q^2)) - 2\lambda\exp(\pi r_h^2)(r_h^2(9\pi(l^2+Q^2)+6) - 10\zeta Q^{3/2}r_h \\ -9(l^2+Q^2)) - 3\pi r_h^2\exp(-2\pi r_h^2)(-4\zeta Q^{3/2}r_h + 3r_h^2 - 3(l^2+Q^2))\Big). \tag{41}$$

In this study, we will analyze the physical behavior of the exponentially corrected Gibbs free energy G_{np}, using Fig. 14. Plots *(a)*, and*(c)*, exhibit similar behavior as observed in the corrected enthalpy. Plot *(b)*, describes the Gibbs free energy relating to the NLED coupling parameter. It demonstrates that the Gibbs free energy of the system remains stable and gradually decreases until it reaches its equilibrium state.

Now, we will examine the thermodynamic stability of our system and the conditions under which phase transitions occur. The specific heat of the BH [67,69] is another quantity used to investigate its local stability. The corrected heat capacity $C_{np} = T(\frac{dS_{np}}{dr_h})(\frac{dr_h}{dT})$ is given by

$$C_{np} = -\frac{2\pi r_h^2\exp\left(-\pi r_h^2\right)\left(\exp\left(\pi r_h^2\right)-\lambda\right)\left(-4\zeta Q^{3/2}r_h + 3r_h^2 - 3\left(l^2+Q^2\right)\right)}{-8\zeta Q^{3/2}r_h + 3r_h^2 - 9\left(l^2+Q^2\right)} \tag{42}$$

The graph of non-perturbed exponential corrected specific heat C_{np}, as a function of horizon radius r_h drawn in Fig. 15. Following inspection of plot *(a)*, it becomes evident that the corrected specific heat for the charged parameter exhibits a consistent negative trend across the entire range of the given domain and shows instability for all values of the charged parameter. The NLED parameter ζ, used to analyze the stability of the specific heat of a small-sized BH at $r_h = 0.8$. It is observed that in the first phase, the specific heat remained stable, while in the second phase, it diverged towards an unstable region, as shown in plot *(b)*. The plot*(c)*, illustrates that the specific heat exhibits stability for small radii and divergence for large radii in the presence of the correction parameter ψ. In the stable region, the specific heat reaches its maximum value when the correction parameter is at its highest.

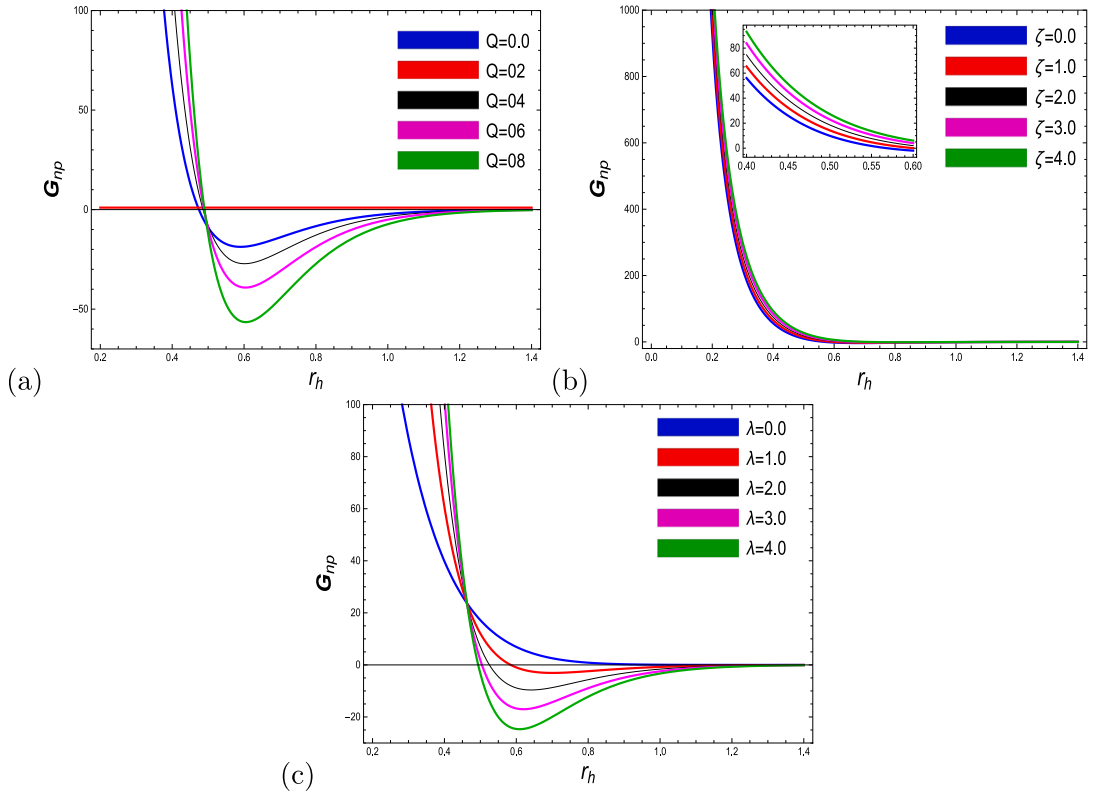

Fig. 14. This figure illustrates the graph of exponentially corrected Gibss free energy as a function of r_h for a specific value of $l = 5$ and for plot (a), we take $\zeta = 0.50$, $\lambda = 0.50$, for (b), $Q = 5$, $\lambda = 1$ and for (c), $Q = 5$, $\zeta = 0.50$.

6. Conclusions

In this paper, we have conducted a comprehensive analysis of the thermodynamic properties exhibited by a charged AdS BH that is coupled with a NLED field. Our investigation primarily focuses on the equilibrium entropy and the modified entropy resulting from thermal fluctuations. Moreover, we have evaluated the thermodynamic potentials through the utilization of equilibrium entropy, particularly focusing on entropy, mass, Hawking temperature, and heat capacity. It has been accepted that quantum corrections arising from thermal fluctuations have a significant impact on the entropy of BHs. For instance, loop quantum gravity and micro-state counting in string theory have both demonstrated the perturbation (logarithmic correction) in entropy. We have observed the impact of logarithmic corrections on the uncorrected thermodynamic parameters of a charged AdS BH with an NLED field. Furthermore, the entropy of a BH receives an exponential correction (non-perturbation) when exclusively considering quantum states restricted to the event horizon as microstates. We have also observed the impact of exponential entropy on the usual entropy of the system. We did a thorough evaluation of a study that compared modified thermodynamic potentials like Helmholtz free energy, total corrected mass pressure, enthalpy, Gibbs free energy, and specific heat. In order to examine the novel points of their physical behavior as well as their significance and impact. The usage of graphical description for analyzing corrected thermodynamic quantities and their corresponding physical aspects are observed. The system is continuous and stable because the modified entropy is positive across all domains. It is worth noting that the validity of the modified first law of BH thermodynamics is also addressed. There is an occurrence of a first-order phase transition that arises from the consideration of logarithmic correction to entropy. Nevertheless, the logarithmic correction does not exert any influence on the second-order phase transition. However, the exponential correction results in a secondary first-order phase transition for the Helmholtz free energy and Gibbs free energy. It is still interesting to expand this work like recent literature [104–110].

Declaration of competing interest

The authors declare that they have no known competing financial interests or personal relationships that could have appeared to influence the work reported in this paper.

Data availability

The data associated with this research paper is available with the corresponding author and can be provided on request.

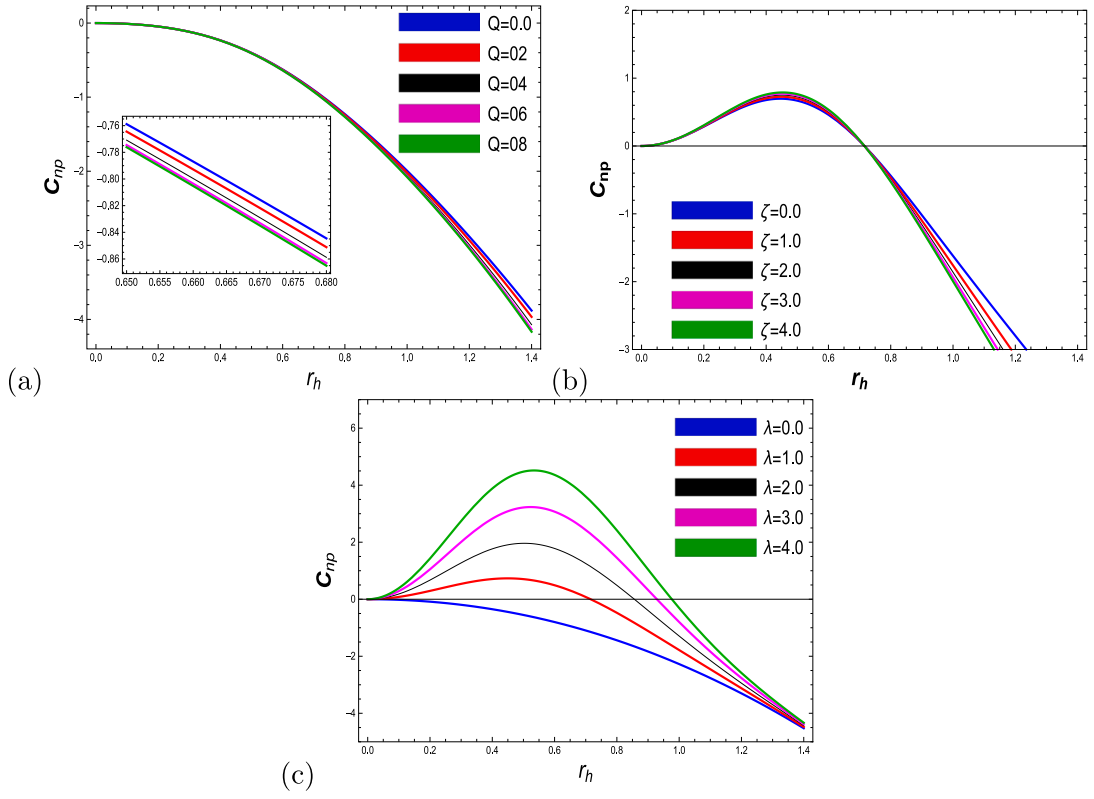

Fig. 15. This figure illustrates the graph of exponentially corrected heat capacity as a function of r_h for a specific value of $l = 5$ and for plot (a), we take $\zeta = 0.20$, $\lambda = 0.50$, for (b), $Q = 5$, $\lambda = 1 = 5$ and for (c), $Q = 2$, $\zeta = 3$.

References

[1] A. Ashtekar, J. Baez, A. Corichi, K. Krasnov, Phys. Rev. Lett. 80 (1998) 904.
[2] A. Strominger, C. Vafa, Phys. Lett. B 379 (1996) 99.
[3] J.D. Bekenstein, Phys. Rev. D 7 (1973) 2333.
[4] J.D. Bardeen, B. Carter, S.W. Hawking, Comm. Math. Phys. 31 (1973) 161.
[5] S.W. Hawking, Comm. Math. Phys. 43 (1975) 199.
[6] G.W. Gibbons, S.W. Hawking, Phys. Rev. D 15 (1977) 2738.
[7] R.M. Wald, Phys. Rev. D 48 (1993) 3427–3431.
[8] M. Visser, Internat. J. Modern Phys. D 12 (2003) 649.
[9] R.M. Wald, Living Rev. Rel. 4 (2001) 6.
[10] F. Simon Ross, arXiv:hep-th/0502195.
[11] S. Vongehr, arXiv:hep-th/9709172.
[12] D. Bak, S.J. Rey, Classical Quantum Gravity 17 (2000) L1.
[13] S.K. Rama, Phys. Lett. B 457 (1999) 268.
[14] J. Sadeghi, B. Pourhassan, F. Rahimi, Can. J. Phys. 92 (12) (2014) 1638–1642.
[15] A. Chatterjee, A. Ghosh, Phys. Rev. Lett. 125 (2020) 041302.
[16] B. Pourhassan, Eur. Phys. J. C 79 (2019) 740.
[17] S. Hemming, L. Thorlacius, J. High Energy Phys. 11 (2007) 086.
[18] R. Gregory, S.F. Ross, R. Zegers, J. High Energy Phys. 09 (2008) 029.
[19] J.V. Rocha, J. High Energy Phys. 08 (2008) 075.
[20] Z.H. Li, B. Hu, R.G. Cai, Phys. Rev. D 77 (2008) 104032.
[21] K. Saraswat, N. Afshordi, J. High Energy Phys. 136 (2020) 04.
[22] R.B. Mann, S.N. Solodukhin, Nuclear Phys. B 523 (1998) 293.
[23] A. Sen, Gen. Relativity Gravitation 44 (2012) 1947.
[24] A. Ashtekar, Lectures on Non-Perturbative Canonical Gravity, World Scientific, Singapore, 1991.
[25] T.R. Govindarajan, R.K. Kaul, V. Suneeta, Classical Quantum Gravity 18 (2001) 2877.
[26] D. Birmingham, S. Sen, Phys. Rev. D 63 (2001) 047501.
[27] Robert B. Mann, J. Hologr. Appl. Phys. 4 (1) (2024) 1–26, http://dx.doi.org/10.22128/jhap.2023.757.1067.
[28] B. Pourhassan, Emmanuel N. Saridakis, Seyed Hossein Hendi, S. Upadhyay, Izzet Sakalli, IJMPD (2024) http://dx.doi.org/10.1142/S0218271823501109.
[29] B. Pourhassan, M. Faizal, Z. Zaz, A. Bhat, Phys. Lett. B 773 (2017) 325.
[30] D. Bak, S.J. Rey, Classical Quantum Gravity 17 (2000) L1.
[31] S.K. Rama, Phys. Lett. B. 457 (1999) 268.
[32] R.K. Kaul, P. Majumdar, Phys. Rev. Lett. 84 (2000) 5255.

[33] S. Hemming, L. Thorlacius, J. High Energy Phys. 086 (2007) 0711.
[34] S. Upadhyay, Phys. Rev. D 95 (2017) 043008.
[35] A. Pourdarvish, J. Sadeghi, H. Farahani, B. Pourhassan, Internat. J. Theoret. Phys. 52 (2013) 3560.
[36] B. Pourhassan, M. Faizal, Eur. Phys. Lett. 111 (2015) 40006.
[37] M. Faizal, B. Pourhassan, Phys. Lett. B 751 (2015) 487.
[38] S. Das, et al., Classical Quantum Gravity 19 (2002) 2355.
[39] M.M. Akbar, S. Das, Classical Quantum Gravity 21 (2004) 1383.
[40] A. Abhay, Lectures on Non-Perturbative Canonical Gravity, World Scientic, 1991.
[41] S. Carlip, Classical Quantum Gravity 17 (2000) 4175.
[42] G. Gour, A.J.M. Medved, Classical Quantum Gravity 20 (2003) 3307.
[43] M. Alishahiha, J. High Energy Phys. 8 (2007) 094.
[44] J. Sadeghi, et al., Eur. Phys. J. C 74 (2014) 2680.
[45] A. Jawad, M.U. Shahzad, Eur. Phys. J. C 77 (2017) 349.
[46] A. Pourdarvish, et al., Internat. J. Theoret. Phys. 52 (2013) 3560.
[47] B. Pourhassan, et al., Gen. Relativity Gravitation 49 (2017) 144.
[48] S. Banerjee, et al., J. High Energy Phys. 2011 (2011) 143.
[49] A. Haldar, R. Biswas, Gen. Relativity Gravitation 50 (2018) 69.
[50] A. Haldar, R. Biswas, Astrophys. Space Sci. 363 (2018) 27.
[51] M. Zhang, Nuclear Phys. B 935 (2018) 170.
[52] C.V. Vishveshwara, Nature 227 (1970) 936.
[53] J. Jing, Q. Pan, Phys. Lett. B 660 (2008) 13.
[54] M. Sharif, A. Khan, Chin. J. Phys. V. 77 (2022) 1130–1144.
[55] M. Sharif, Z. Akhtar, Phys. Dark Univ. 29 (2020) 100589.
[56] M. Sharif, A. Khan, Chin. J. Phys. V. 77 (2022) 1885–1902.
[57] G. Abbas, R.H. Ali, Chin. Phys. C 47 (2023) 065103.
[58] G. Abbas, R.H. Ali, Eur. Phys. J. C 83 (2023) 407.
[59] R.H. Ali, G. Abbas, Chinese J. Phys. (2023) 0577–9073, http://dx.doi.org/10.1016/j.cjph.2023.07.008.
[60] Behnam Pourhassan, Hoda Farahani, Farideh Kazemian, Izzet Sakalli, Sudhaker Upadhyay, Dharm Veer Singh, Phys. Dark Univ. 44 (2024) 101444.
[61] B. Pourhassan, M. Dehghani, M. Faizal, S. Dey, Classical Quantum Gravity 38 (2021) 105001.
[62] A. Ashtekar, World Scientific, vol. 06, Singapore, 1991.
[63] A. Ghosh, P. Mitra, Phys. Lett. B 734 (2014) 49.
[64] A. Dabholkar, J. Gomes, S. Murthy, J. High Energy Phys. 03 (2015) 074.
[65] J. Maldacena, Int. J. Theor. Phys. 38 (1999) 1113.
[66] S. Murthy, B. Pioline, J. High Energy Phys. 09 (2009) 022.
[67] A. Dabholkar, J. Gomes, S. Murthy, J. High Energy Phys. 04 (2013) 062.
[68] B. Pourhassan, M. Dehghani, S. Upadhyay, I. Sakall, D.V. Singh, Modrn. Phys. Lett. A 37 (2022) 2250230.
[69] S. Masood, A.S. Bukhari, B. Pourhassan, H. Aounallah, Li-Gang Wang, http://dx.doi.org/10.48550/arXiv.2304.00940.
[70] D. Rasheed, High Energy Phys. (1997).
[71] N. Breton, Smarr formula for black holes with non-linear electrodynamics, Gen. Relativity Gravitation 37 (2005) 643.
[72] W. Yi-Huan, Chin. Phys. B 19 (2010) 090404.
[73] M. Novello, E. Goulart, J.M. Salim, S.E. Perez Bergliaffa, Classical Quantum Gravity 24 (2007) 3021.
[74] M. Novello, Aline N. Araujo, J.M. Salim, arXiv:0802.1875.
[75] C.S. Camara, J.C. Carvalho, M.R. De Garcia Maia, Internat. J. Modern Phys. D 16 (2007) 427.
[76] M. Novello, S.E. Perez Bergliaffa, J. Salim, Phys. Rev. D 69 (2004) 127301.
[77] M. Novello, S.E. Perez Bergliaffa, Phys. Rep. 463 (2008) 127.
[78] M. Novello, E. Goulart, J.M. Salim, S.E. Perez Bergli-affa, Classical Quantum Gravity 24 (2007) 3021.
[79] V.A. De Lorenci, R. Klippert, M. Novello, J.M. Salim, Phys. Rev. D 65 (2002) 063501.
[80] K.A. Bronnikov, I.G. Dymnikova, E. Galaktionov, Classical Quantum Gravity 29 (2012) 095025.
[81] S.V. Bolokhov, K.A. Bronnikov, M.V. Skvortsova, Classical Quantum Gravity 29 (2012) 245006.
[82] K.A. Bronnikov, K.A. Baleevskikh, M.V. Skvortsova, Phys. Rev. D 96 (2017) 124039.
[83] S. Nojiri, S.D. Odintsov, Phys. Rev. D 96 (2017) 104008.
[84] C. Gao, Y. Lu, S. Yu, Y. Shen, Phys. Rev. D 97 (2018) 104013.
[85] S. Gunasekaran, R.B. Mann, D. Kubiznak, J. High Energ. Phys. 11 (2012) 110.
[86] S.H. Mazharimousavi, Phys. Lett. B 841 (2023) 137948.
[87] S.H. Mazharimousavi, Phys. Lett. B 841 (2023) 137948.
[88] L.F. Abbott, S. Deser, Nuclear Phys. B 195 (1982) 76.
[89] S.H. Hendi, B. Eslam Panah, S. Panahiyan, A. Sheykhi, Phys. Lett. B 767 (2017) 214–225.
[90] J.D. Bekenstein, Phys. Rev. D 9 (1974) 3292.
[91] S. Upadhyay, Gen. Relativity Gravitation 50 (2018) 128.
[92] B. Pourhassan, H. Farahani, S. Upadhyay, Internat. J. Modern Phys. A 34 (2019) 1950158.
[93] N. Ialam, P.A. Ganai, S. Upadhyay, J. PTEP 2019 (2019).
[94] M. Everton, C. Abreu, J.A. Neto, Eur. Phys. J. C. 80 (2020) 776.
[95] B. Pourhassan, S. Upadhyay, Eur. Phys. J. Plus. 136 (2021) 311.
[96] X. Chen, X. Huang, J. Chen, Y. Wang, Gen. Rel. Grav. 53 (2021).
[97] A. Jawad, Classical Quantum Gravity 37 (2020) 185020.
[98] S. Pal, R. Biswas, Int. J. Theo. Phys. 61 (2022).
[99] S. Upadhyay, S.H. Hendi, S. Panahiyan, B.E. Panah, Prog. Theor. Exp. Phys 2018 (2018) 093E01.
[100] O. Okcu, E. Aydiner, Phys. gen-Ph (2017).
[101] A. Jawad, S. Chaudhry, K. Jusufi, Iran J. Sci. Technol. Trans. 46 (2022).
[102] B. Pourhassan, M. Faizal, J. High Energy Phys. 2021 (2021) 1–18.
[103] B. Pourhassan, S.S. Wani, S. Soroushfar, M. Faizal, J. High Energy Phys. 2021 (2021) 27.
[104] B. Pourhassan, I. Sakalli, Chinese J. Phys. 79 (2022) 322–338.
[105] B. Pourhassan, M. Faizal, S. Upadhyay, L. Al Asfar, Eur. Phys. J. C 77 (2017) 555.
[106] B. Pourhassan, M. Faizal, U. Debnath, Eur. Phys. J. C 76 (2016) 145.
[107] N. ul Islam Rather, P.A. Ganai, J. Hologr. Appl. Phys. 3 (3) (2023) 23–36.
[108] S. Upadhyay, N. ul Islam, P.A. Ganai, J. Hologr. Appl. Phys. 2 (1) (2022) 25–48.
[109] R.C. Delgado, J. Hologr. Appl. Phys. 3 (1) (2023) 39–48.
[110] S. Saghafi, K. Nozari, J. Hologr. Appl. Phys. 2 (2) (2022) 31–38.